The effect of Si-nanocrystal size distribution on Raman spectrum

Weiwei Ke, Xue Feng,[a)] and Yidong Huang
State Key Lab. of Integrated Optoelectronics, Department of Electronic Engineering, Tsinghua University, Beijing 100084, China

The effect of Si-nanocrystal (Si-nc) size distribution on Raman spectrum is studied in detail within the framework of a phonon confinement model. It is found that size distribution has little effect on Raman frequency shift, but greatly affects the width and shape of Raman spectrum. Si-nc Raman spectrum can be well explained by considering the size distribution. Furthermore, a set of simple relationships between Raman frequency shift/full width at half maximum (FWHM) and size distribution is set up based on the framework of a modified phonon confinement model, which can be applied to calculate Si-nc size distribution from the Raman spectrum. © 2011 American Institute of Physics. [doi:10.1063/1.3569888]

I. INTRODUCTION

Si-nanocrystals (Si-nc) have attracted intense attention in recent years due to many potential applications, such as silicon-based light sources,[1,2] biological labeling,[3,4] and non-volatile memory devices,[5,6] among others. For all these applications, clarifying the size distribution of Si-nc is very important. Since the Raman spectrum was found to be greatly affected by Si-nc size,[7] it has been employed to determine Si-nc size distribution by many authors.[8,9] Compared with other conventional methods, such as transmission electron microscopy (TEM) and x-ray diffraction, Raman scattering is much preferred for its nondestructive measuring, small specimen quantity requirement, and short measurement time.

The phonon confinement model (PCM),[10] originally proposed by Richter, Wang, and Ley (hereafter this original model is referred to as the RWL model), has been widely used to explain the Si-nc Raman spectrum[11] and determine their size distribution.[8,9] However, the RWL model can only serve as a qualitative analysis of the practical Raman frequency shift.[12] An improved model proposed by Faraci *et al.*[12] overcomes such a problem, but the Raman spectrum width predicted by this model was far less than experimental results. Moreover, the effect of Si-nc size distribution on the Raman spectrum, which is critical to the application of Si-nc size distribution calculation, was still not studied in detail.

In this paper, the effect of Si-nc size distribution on the Raman spectrum is studied in detail with both the RWL model and Faraci's model. It is found that size distribution has little effect on the Raman frequency shift, but greatly affects the width and shape of the Raman spectrum. Considering the size distribution, Faraci's model can well explain both the Raman frequency shift and the full width at half maximum (FWHM) while the RWL model can only explain the FWHM. Based on the framework of Faraci's model, a set of simple relationships between Raman frequency shift/

FWHM and size distribution is set up and applied to calculate Si-nc size distribution from the Raman scattering spectrum.

II. THEORY

According to the assumption of PCM,[10] the phonon wave function of a single Si-nc is the product of the wave function in an infinite crystal and a weighting function $W(\mathbf{r}, D)$, where D is the diameter of the Si-nc. $W(\mathbf{r}, D)$ describes the Si-nc phonon confinement effect and usually forces phonon wave function to vanish beyond the Si-nc boundary. In this paper, a sinc function

$$W(r, D) = \begin{cases} \text{sinc}(2r/D), & r \le D/2 \\ 0, & r > D/2 \end{cases} \quad (1)$$

is used. It equals 0 just at the Si-nc boundary and could describe the phonon confinement effect well.[13]

The Raman spectrum of a Si-nc with diameter D can thus be written as[14]

$$I(\omega, D) \propto [n(\omega) + 1] \int \frac{|C(\mathbf{q}, D)|^2}{[\omega - \omega(\mathbf{q})]^2 + (\Gamma_0/2)^2} d^3\mathbf{q} \quad (2)$$

where $n(\omega) + 1$ is the Bose–Einstein factor, $C(\mathbf{q}, D)$ is the Fourier coefficients of $W(\mathbf{r}, D)$, Γ_0 is the Raman natural linewidth of bulk Si, and $\omega(\mathbf{q})$ is the corresponding phonon dispersion curve. In this paper, Γ_0 is set as 3 cm^{-1} and $\omega(\mathbf{q})$ is expressed as

$$\omega(q_r) = \sqrt{522^2 - \frac{126100 q_r^2}{|q_r| + 0.53}}, \quad (3)$$

which was proposed by Paillard[14] based on the Brout sum, and q_r is the reduced phonon wave vector. There are other phonon dispersion expressions proposed in publications and some effects of applying different ones will be discussed in Sec. III B1.

In the RWL model, all phonons in the Brillouin zone are considered as Raman active. Thus the integral limits of Eq. (2) are extended to the entire Brillouin zone. This

---

a)Author to whom correspondence should be addressed. Electronic mail: x-feng@tsinghua.edu.cn. Room 113, Weiqing Building, Tsinghua University, Beijing, 100084 China.

assumption has been widely used to explain the Si-nc Raman spectrum and calculate Si-nc size distribution, although it can explain only the shift trend of the practical Raman frequency. Faraci et al.[12] made a different assumption in their improved model to overcome such a problem. While the requirements of energy and momentum conservation and the uncertainty principle are considered, only phonons with wave vector in the range $[(2\pi-1)/D, (2\pi+1)/D]$ should be treated as Raman active. In this paper, the Si-nc size distribution effects on Raman spectrum will be considered with both models.

Equation (2) can only represent the Raman spectrum of Si-nc with uniform size. When the size distribution $f(D)$ is considered, the Raman spectrum can be written as[9]

$$I(\omega) \propto \int I(\omega, D) f(D) dD. \tag{4}$$

Here, a lognormal function, which has been widely used for practical samples, is adopted to describe Si-nc size distribution

$$f(D) \propto \exp\left(-\frac{(\ln(D/D_0))^2}{2\sigma^2}\right) \tag{5}$$

where D_0 is the most probable diameter and σ is a parameter used to describe the size distribution width.

III. RESULTS

With the theory outlined above, Raman scattering spectra of Si-ncs with some different size distributions are calculated and summarized as follows.

A. Size distribution effects on Raman spectrum

Figures 1(a) and 1(b) are the representative results for Si-ncs with D_0 of 10 nm and 2 nm calculated with the RWL model and Faraci's model, respectively. Parameter σ is varied from 0–0.4 with a step of 0.1. $\sigma = 0$ represents that all Si-ncs are of uniform size, while $\sigma = 0.4$ represents a rather wide size distribution. It should be noted the FWHM of lognormal distribution [Eq. (5)] is proportional to 2.35 $D_0\sigma$ approximately, so for $\sigma = 0.4$, the FWHM nearly equals D_0 itself.

With $D_0 = 10$ nm, the calculated Raman spectrum (for both models) are almost unaffected by size distribution and almost the same as the bulk Si Raman spectrum for all σ values. This phenomenon is mainly due to the weak phonon confinement effect of large Si-ncs. In contrast, with $D_0 = 2$
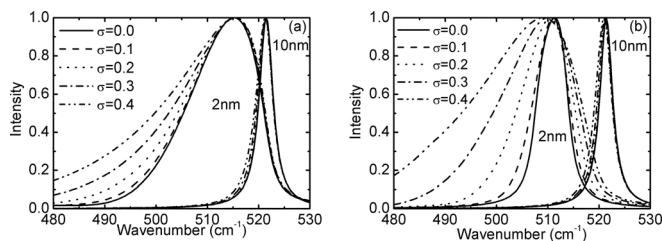
nm, the influence of the size distribution is significant. The Raman spectrum broadens along with the increase of σ, which is more remarkable in Faraci's model. Furthermore, Faraci's model predicts broadening on both sides of the Raman spectrum while the RWL model predicts broadening only on the left side. Besides the broadening of the Raman spectrum, one should note a large Raman frequency shift for Si-ncs with D_0 of 2 nm. However, the size distribution (parameter σ) has little effect on this frequency shift, especially for the RWL model.

In order to get deeper insight into the phenomena described above, the peak shift, FWHM, and shape of the Raman spectrum of Si-ncs with $D_0 = 1.5$–10 nm and $\sigma = 0$–0.4 are calculated and summarized in Figs. 2, 3, and 4. For each figure, parts (a) and (b) are results calculated with the RWL model and with Faraci's model, respectively. Some experimental data are also reprinted for comparison.[9,14–16] Here, Raman frequency shift is defined as $\Delta\omega = \omega_0 - \omega_{nc}$, where ω_0 and ω_{nc} are the Raman frequency of bulk Si and Si-ncs, respectively. In order to describe the asymmetrical shape of the Raman spectrum, the low and high wavenumbers at half maximum (LWHM and HWHM in short) are adopted in Fig. 4. These two values are read artificially from Raman spectra on papers. With this definition, FWHM is thus HWHM – LWHM.

As shown in Fig. 2, size distribution has little effect on the calculated Raman frequency shift for both models. In other words, the Raman frequency shift is mainly determined by the Si-ncs with the most probable size D_0 which denominate the samples in magnitude. In contrast, size distribution greatly affects the width and the shape of the Raman spectrum (Figs. 3 and 4). This is reasonable because the number of Si-ncs with different sizes increases along with the broadening of size distribution and that leads to the increase of Raman scattering frequency components. These phenomena are more remarkable in Faraci's model than in the RWL model. That can be explained by the assumption of which kind of phonons contributes to the Raman scattering process in these two models. For Faraci's model, only one kind of phonons (with wave vectors around $2\pi/D$) is Raman active, while all phonons in the entire Brillouin zone are involved for the RWL model. Along with the broadening of Si-nc size distribution, the variation in kinds of wave vectors of the Raman active phonons is more significant in Faraci's model, so Faraci's model is more sensitive to Si-nc size distribution.

The RWL model can explain FWHM no matter whether size distribution is considered. Also, Faraci's model can

FIG. 1. Calculated Raman spectra of Si-ncs with D_0 of 10 nm and 2 nm with RWL model (a) and Faraci's model (b).
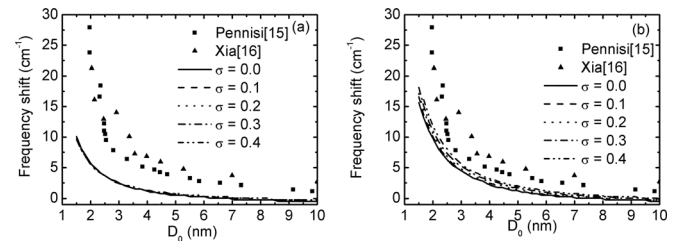

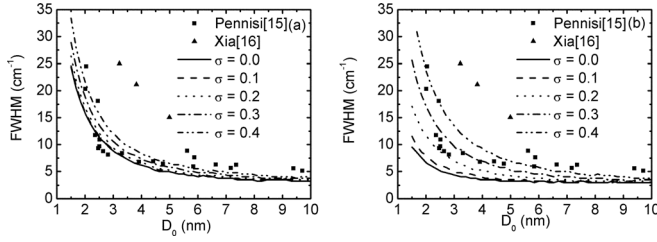FIG. 2. Calculated Raman frequency shift with RWL model (a) and Faraci's model (b).

FIG. 3. Calculated FWHM of Raman spectrum with RWL model (a) and Faraci's model (b).

explain not only FWHM well (Fig. 3, $\sigma = 0.2$–0.3 for example, and these values are consistent with those determined by other methods, such as TEM.[9,15]) but also explains the frequency shift when size distribution is considered. Therefore Faraci's model is preferred for explaining Si-nc Raman spectrum. In the following sections, only Faraci's model will be adopted for detailed discussion.

B. Analytic results based on Faraci's model

In order to explain the experimental results of the Si-nc Raman spectrum or to determine Si-nc size distribution, a calculation or a fitting of a double integral combined with Eqs. (2) and (4) usually is needed. However, this section will show that there are analytic expressions for the Raman frequency shift and FWHM based on the framework of Faraci's model with Si-nc size distribution. These expressions can not only simplify the calculation process of Si-nc size distribution, but also reveal the simple and clear relationships between the Raman frequency shift/FWHM and Si-nc size distribution.

1. Raman frequency shift

When Si-nc size distribution is not considered, the Raman spectrum can be calculated with Eq. (2), where the integral range is from $(2\pi - 1)/D$ to $(2\pi + 1)/D$. This integral is a weighted summation of Raman spectra of phonons with wave vector q. Each Raman spectrum has an identical Lorentzian shape with a central frequency of $\omega(q)$ and width of Γ_0, and the corresponding weight factor is $|C(q, D)|^2 q^2$. This process is illustrated in Fig. 5 (Si-nc with $D_0 = 2$ nm). The high dot-dash line is the final Raman spectrum and the low lines are Raman spectra of single Raman active phonons with weighted factors.

It can be seen that the Raman frequency is nearly equal to that of the central Lorentzian curve, which corresponds to the phonon with wave vector $2\pi/D$. That is,
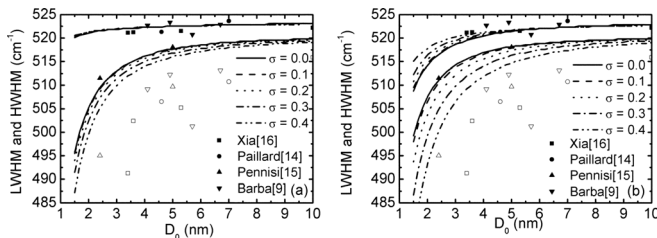

FIG. 4. Calculated LWHM and HWHM of Raman spectrum with RWL model (a) and Faraci's model (b). Solid points and hollow points are the LWHM and HWHM of experimental results, respectively.
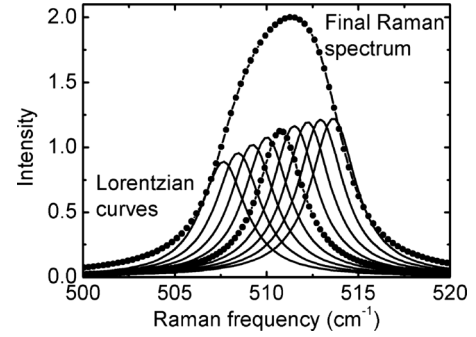

FIG. 5. The weighted summation of integration of Eq. (2). The lower dot-dash line is the Lorentzian curves in the center of integral range.

$$\omega_{nc}(D) = \omega(2\pi/D), \quad (6)$$

where $\omega(q)$ is the phonon dispersion curve of bulk Si.

The generality and validation of Eq. (6) can be understood by following two factors. First, the weight factor $|C(q, D)|^2 q^2$ is nearly a constant in the integral range from $(2\pi - 1)/D$ to $(2\pi + 1)/D$. As shown in Fig. 6(a) (axis x is reduced as $qD/2$ to exclude the effect of size D), the variation is less than 15% compared with their average value. Thus, the final Raman spectrum can be regarded as a simple summation of the Lorentzian curves. Second, the central frequencies of these Lorentzian curves $\omega(q)$ are nearly symmetrical compared with the central one in the whole integral range, which would make the final Raman frequency almost equal to that of the central one. The symmetry can be understood by the phonon dispersion relation of bulk Si. Figure 6(b) is the typical phonon dispersion curve where the x axis is the reduced phonon wave vector $q_r = q/(2\pi/a)$ and $a = 0.543$ nm is the lattice parameter of Si. The key point is that the integral range $a/(\pi D)$ is narrow in Faraci's model. For example, $a/(\pi D)$ are 0.085 and 0.017 for D of 2 nm and 10 nm, respectively. Within such a narrow range, the dispersion curve $\omega(q)$ could be treated as linear. Thus the central frequency of the Lorentzian curve in Eq. (2) shifts linearly along with wave vector q.

As a result, the Raman frequency shift of Si-nc with diameter D can be written as

$$\Delta\omega(D) = \omega_0 - \omega(2\pi/D), \quad (7)$$

where ω_0 is the Raman frequency of bulk Si. By applying the dispersion curve of Eq. (3) into Eq. (7), the Raman frequency shift could be expressed as
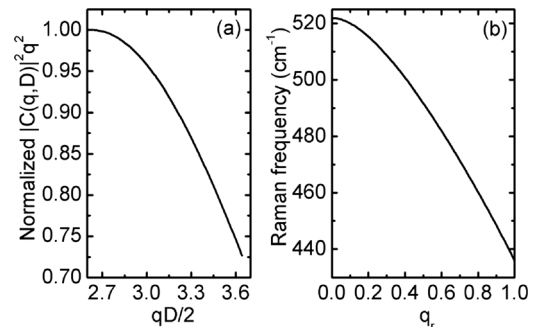

FIG. 6. (a) The normalized weighted factor $|C(q, D)|^2 q^2$, (b) the typical phonon dispersion curve of bulk Si.

$$\Delta\omega(D) = \frac{120.8}{a/D + 0.53} \times (a/D)^2. \qquad (8)$$

Figure 7 shows the results of the Raman frequency shift calculated with the integral formula of Eq. (2) and the analytic formula of Eq. (8). It can be seen that the difference is negligible.

With the bond-polarizability model,[17] it has been proposed that the Raman frequency shift could be expressed as

$$\Delta\omega(D) = A(a/D)^{\gamma}. \qquad (9)$$

One could find that Eqs. (8) and (9) are very similar. In fact, an identical form of $\omega(D) = 0.2\,\omega_0(a/D)^2$ could be deduced by choosing the phonon dispersion relationship form[9] of $\omega(q_r) = \omega_0(1 - 0.20q_r^2)$. So these two different models may come to the same conclusion.

When Si-nc size distribution is considered, the Raman frequency shift almost remains the same, as shown in Sec. III A. Thus, the Raman frequency shift of Si-nc can always be written as Eq. (7) in Faraci's model.

2. Raman spectrum FWHM

As with the Raman frequency shift, there is an analytic approximation of the Raman spectrum FWHM. Because only one kind of phonon (wave vector around $2\pi/D$) is Raman active for Si-nc with a given size, the FWHM of the final Raman spectrum can be regarded as a coupling of two parts. One is the intrinsic width due to the given size and the other one is the width due to size distribution. Two critical sizes at which the size distribution value falls to half maximum are

$$D_{1,2} = D_0 \exp(\pm\sqrt{2\ln 2}\sigma). \qquad (10)$$

The broadening of Si-nc Raman spectrum due to size distribution could be approximately regarded as the difference of Raman frequencies of Si-nc with these two critical sizes. By expanding dispersion curve to the second order term $\omega(q_r) = \omega_0 + q_r^2 d\omega^2/dq_r^2$ (the first order term is neglectable as the form given by[9]), these two corresponding frequencies are

$$\omega(D_{1,2}) = \omega_0 + \frac{d\omega^2}{dq_r^2}\left(\frac{a}{D_0}\right)^2 \exp(\pm 2\sqrt{2\ln 2}\sigma) \qquad (11)$$
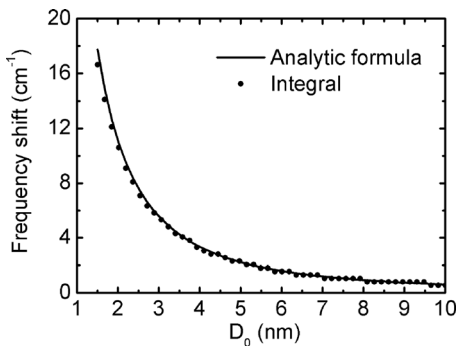
where $(a/D_0)^2 d\omega^2/dq_r^2$ is just the approximation of Raman frequency shift $\Delta\omega(D_0)$. Thus, the FWHM can be written as

$$\Omega \approx |\omega(D_1) - \omega(D_2)| \approx \Delta\omega(D_0) \times 4\sqrt{2\ln 2}\sigma + \Gamma_0, \qquad (12)$$

where Γ_0 is the natural linewidth of the bulk Si Raman spectrum, and it is attached artificially in Eq. (12) to compensate for the intrinsic width of the Si-nc Raman spectrum.

Figure 8 shows the results of Raman FWHM calculated with the integral formula of Eq. (4) (small dots) and the analytic formula of Eq. (12) (solid lines), where σ is 0.1, 0.2, 0.3, and 0.4. It can be seen that the difference between them is negligible. In our calculation, we find that Eq. (12) fails while σ is very small (e.g., $\sigma = 0$ leads to $\Omega = \Gamma_0$). The reason is that the intrinsic width of the Si-nc Raman spectrum dominates in such cases. However, as shown in Fig. 8, the analytic result is very precise while σ is larger than 0.1.

As shown by Eq. (12), the increase of the Raman spectrum FWHM is simply proportional to the width of the size distribution and the Raman frequency shift.

C. Determining Si-nc size distribution with the Raman spectrum

The analytic results we obtained establish a set of simple and clear relationships between the Raman frequency shift/FWHM and Si-nc size distribution. An important application of these results is to calculate Si-nc size distribution with the Raman spectrum.

With Eqs. (7) and (12), when the Raman frequency shift $\Delta\omega$ and FWHM Ω of samples are obtained from experiments, the parameters D_0 and σ of Si-nc size distribution then can be calculated as

$$\begin{cases} D_0 = a/\omega^{-1}(\omega_0 - \Delta\omega) \\ \sigma = \frac{\Omega - \Gamma_0}{4\sqrt{2\ln 2}\Delta\omega} \end{cases}, \qquad (13)$$

where a is the lattice parameter of bulk Si, ω_0 is its Raman frequency, Γ_0 is its Raman natural linewidth and $\omega^{-1}(\cdot)$ is the inverse function of its phonon dispersion curve. While the dispersion curve is given by Eq. (3), $\omega^{-1}(\cdot)$ is given by

FIG. 7. Calculated Raman frequency shift with integration of Eq. (2) and analytic formula of Eq. (8).
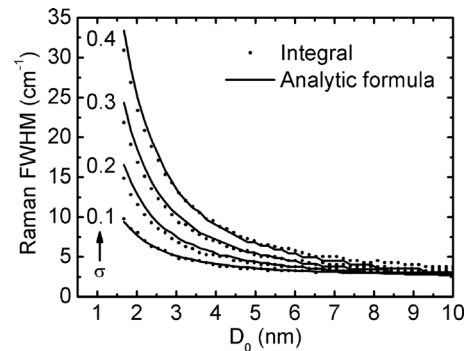

FIG. 8. Calculated FWHM of Raman spectrum with full integration of Eq. (4) and analytic formula of Eq. (12).

$$\omega^{-1}(\omega_{nc}) = q_r = \frac{(522^2 - \omega_{nc}^2) + \sqrt{(522^2 - \omega_{nc}^2)^2 + 267332(522^2 - \omega_{nc}^2)}}{252200}.$$

(14)

When the dispersion curve[9] is $\omega(q_r) = \omega_0(1 - 0.20q_r^2)$, $\omega^{-1}(\cdot)$ can be simple:

$$\omega^{-1}(\omega_{nc}) = q_r = \sqrt{5(1 - \omega_{nc}/\omega_0)}.$$

(15)

From Eq. (13), it can be seen that D_0 is only determined by the Raman frequency shift, and σ is determined by both the Raman frequency shift and FWHM. Therefore the size distribution of Si-nc can be easily calculated with Raman measurement. The validation of Eq. (13) can be experimentally verified by other measurement methods, such as TEM, and related work is ongoing.

IV. DISCUSSION

It can be seen that PCM can be used to explain the Si-nc Raman spectrum well when size distribution is considered. However, there are still some differences between the theoretical results and experiments, which can be seen clearly in Figs. 2, 3, and 4.

For example, the predicted Raman frequency shift is slightly lower than that in the experimental data. As we have shown, such deviation cannot be explained by the size distribution. One possible reason is that the real phonon confinement effect of Si-nc is stronger than the assumption. The phonon wave function could vanish before it reaches the boundary of Si-nc. Stronger phonon confinement leads to a larger shift of Raman frequency. Other influencing factors may be the surface phonon scattering (especially for the small size Si-nc) and the temperature effect of Raman scattering. In order to include the surface effect in the framework of PCM, a possible method is replacing the bulk Si phonon dispersion curve with a modified one since the dispersion curve directly determines the Raman frequency shift, as shown in Sec. III B 1.

Besides the phonon confinement and surface effect, an important factor that can lead to spectrum broadening is amorphous Si-ncs in samples. It has been well known that amorphous Si has a very wide Raman spectrum and small Si-ncs may hardly crystallize even at high temperatures. These small and amorphous Si-ncs can be critical in applications since they show high luminescence efficiency and can influence the growth dynamics of Si-ncs. As shown in Fig. 4, LWHM, which can be strongly influenced by small Si-ncs and amorphous Si, deviates from experimental results significantly. By including the effect of amorphous Si-ncs, the shape of the Raman spectrum may be explained much better.

V. CONCLUSION

In conclusion, the effect of Si-nc size distribution on Raman spectrum is studied in detail with the RWL model and Faraci's model. It is found that size distribution has little effect on the Raman frequency shift, but greatly affects the width and shape of the Raman spectrum. When considering the size distribution, Faraci's model is preferable for explaining the Si-nc Raman spectrum, including both frequency shift and FWHM. Based on the framework of this model, a set of simple and analytic relationships between Raman frequency shift/FWHM and size distribution is set up, which may simplify the calculation of Si-nc size distribution. It is also found that the Raman frequency shift is related to the dispersion curve of bulk Si, and the increase of the Raman spectrum FWHM is proportional to the width of the size distribution and the Raman frequency shift.

[1]G. Y. Sung, N.-M. Park, J.-H. Shin, K.-H. Kim, T.-Y. Kim, K. S. Cho, and C. Huh, IEEE J. Sel. Top. Quantum Electron. **12**, 1545 (2006).

[2]Y. H. Pai, C. H. Chang, and G. R. Lin, IEEE J. Sel. Top. Quantum Electron. **15**, 1387 (2009).

[3]F. Erogbogbo, K. T. Yong, I. Roy, G. Xu, P. N. Prasad, and M. T. Swihart, ACS Nano **2**, 873 (2008).

[4]Z. F. Li and E. Ruckenstein, Nano Lett. **4**, 1463 (2004).

[5]S. Choi, H. Yang, M. Chang, S. Baek, H. Hwanga, S. Jeon, J. Kim, and C. Kim, Appl. Phys. Lett. **86**, 251901 (2005).

[6]T. Y. Chiang, T. S. Chao, Y. H. Wu, and W. L. Yang, IEEE Electron Device Lett. **29**, 1148 (2008).

[7]I.H. Campbell and P.M. Fauchet, Solid State Commun. **58**, 739 (1986).

[8]D. Ristić, M. Ivanda, and K. Furić, J. Mol. Struct. **924-926**, 291 (2009).

[9]D. Barba, F. Martin, and G. G. Ross, Nanotechnology. **19**, 115707 (2008).

[10]H. Richter, Z. P. Wang, and L. Ley, Solid State Commun. **39**, 625 (1981).

[11]S. Hernández, A. Martínez, P. Pellegrino, Y. Lebour, B. Garrido, E. Jordana, and J. M. Fedeli, J. Appl. Phys. **104**, 044304 (2008).

[12]G. Faraci, S. Gibilisco, P. Russo, A. R. Pennisi, and S. L. Rosa, Phys. Rev. B. **73**, 033307 (2006).

[13]J. Zi, K. Zhang, and X. Xie, Phys. Rev. B. **55**, 9263 (1997).

[14]V. Paillard, P. Puech, M. A. Laguna, R. Carles, B. Kohn, and F. Huisken, J. Appl. Phys. **86**, 1921 (1999).

[15]G. Faraci, S. Gibilisco, P. Russo, A. R. Pennisi, G. Compagnini, S. Battiato, R. Puglisi, and S. L. Rosa, Eur. Phys. J. B. **46**, 457 (2005).

[16]H. Xia, Y. L. He, L. C. Wang, W. Zhang, X. N. Liu, X. K. Zhang, D. Fang, and H. E. Jackson, J. Appl. Phys. **78**, 6705 (1995).

[17]J. Zi, H. Büscher, C. Falter, W. Ludwig, K. Zhang, and X. Xie, Appl. Phys. Lett. **69**, 200 (1996).